Pattern formation in phase-separating alloys with cubic symmetry

Hiraku Nishimori and Akira Onuki
Research Institute for Fundamental Physics, Kyoto University, Kyoto 606, Japan
(Received 2 January 1990)

Computer simulations of spinodal decomposition in alloys are performed in two dimensions using a simple dynamic model which takes into account the elastic effect. We examine the domain morphology in late stages of the phase separation in the presence of cubic elastic anisotropy and external stresses.

A numerous number of experimental data have been accumulated on the morphologies of modulated structures in two-phase cubic alloys in the metallurgical literature.[1] In such alloys we observe somewhat ordered arrays of anisotropic domains in late stages of the phase separation. In his linear theory, Cahn[2] examined effects of the cubic elastic anisotropy on the phase transition and found that spinodal decomposition should be triggered by concentration fluctuations varying in the "softest" directions on lowering of the temperature. Domains then tend to grow on the habit planes which are perpendicular to the softest directions. Furthermore, when external stresses are applied, more varied morphologies have been observed in a number of experiments[3] and a Monte Carlo simulation.[4] As a simple typical case, lamellar structures can be selected if the applied stress is uniaxial along [100]. We generally expect complicated competition between the inherent cubic anisotropy and external stresses. Obviously the elastic effect is crucial in these phenomena.[5] However, most theories of phase separations in the physical literature have neglected elastic interactions,[6,7] and its theoretical study is still premature at present.[5] Recently one of the authors[8,9] has proposed a Ginzburg-Landau theory for systematic analysis of the elastic effect in alloys. The purposes here are to demonstrate emergence of the modulated structures from our dynamic model and to study effects of external stresses on the domain morphology.

First we briefly explain our model for cubic solids under the coherent condition.[8,9] We assume that the concentration field c is coupled with the strain tensor $\partial u_i/\partial x_j$ in the free energy F in the form

$$F=\int d\mathbf{r}\,[f(c)+\tfrac{1}{2}(\nabla c)^2+ac(\nabla\cdot\mathbf{u})+f_{\rm el}]\,, \tag{1}$$

where $f(c)$ is the Ginzburg-Landau free-energy density for c, c is measured from some reference value, and a is the coupling constant between c and $\nabla\cdot\mathbf{u}$. The $f_{\rm el}$ is the usual elastic free energy measured from the reference state in which $c=0$,

$$f_{\rm el}=\tfrac{1}{2}(C_{11}-C_{12})\sum_i\left(\frac{\partial}{\partial x_i}u_i\right)^2 +\tfrac{1}{2}C_{12}(\nabla\cdot\mathbf{u})^2+\tfrac{1}{4}C_{44}\sum_{i\neq j}u_{ij}^2\,, \tag{2}$$

where $u_{ij}\equiv\partial u_i/\partial x_j+\partial u_j/\partial x_i$ and C_{ij} are the stiffness constants. The domain morphology can be influenced by external stresses only when the two phases have different stiffness constants as long as $f_{\rm el}$ is composed of terms bilinear in $\mathbf{u}$.[8] To take into account such an effect we allow C_{ij} to depend linearly on c as

$$C_{ij}=C_{ij}^0+cC_{ij}^1\,, \tag{3}$$

where C_{ij}^0 and C_{ij}^1 are constants. The stress tensor σ_{ij} is given by

$$\sigma_{ii}=ac+C_{11}\frac{\partial}{\partial x_i}u_i+C_{12}\left(\nabla\cdot\mathbf{u}-\frac{\partial}{\partial x_i}u_i\right), \tag{4}$$

$$\sigma_{ij}=C_{44}\left(\frac{\partial}{\partial x_i}u_j+\frac{\partial}{\partial x_j}u_i\right)\ \text{for } i\neq j\,. \tag{5}$$

Since we have assumed that c is a conserved variable, the relaxation time of c is much slower than that of $\mathbf{u}$ at long wavelengths and we may assume that the elastic field instantaneously relaxes to adjust to a given concentration field. This is the condition of mechanical equilibrium,

$$\delta F/\delta u_i=-\sum_j\frac{\partial}{\partial x_j}\sigma_{ij}=0\,. \tag{6}$$

The dynamic equation for c is assumed to be of the diffusion type,

$$(\partial/\partial t)c=\lambda\nabla^2(\delta F/\delta c)=\lambda\nabla^2(f'-\nabla^2c+\mu_{\rm el})\,, \tag{7}$$

where λ is the kinetic coefficient, $f'=\partial f/\partial c$, and $\mu_{\rm el}$ is the elastic part of the chemical potential given by $\mu_{\rm el}=a\nabla\cdot\mathbf{u}+\partial f_{\rm el}/\partial c$ from (1).

Next we make the linear stability analysis. Expecting only small fluctuations, we assume that c is composed of a homogeneous average and a small sinusoidal deviation, $c=\bar{c}+c_1\exp(i\mathbf{k}\cdot\mathbf{r})$. The strain is then of the form

$$\partial u_i/\partial x_j=A_{ij}+ik_ju_{1i}\exp(i\mathbf{k}\cdot\mathbf{r})\,,$$

where the average strain $A_{ij}=\langle\partial u_i/\partial x_j\rangle$ arises from the external stress imposed at the boundary. From (6) we may readily calculate the small displacement u_{1i} in terms of the concentration deviation c_1 to obtain the linearized version of (7),

$$(\partial/\partial t)c_1=-\lambda k^2[f''+k^2+\tau_{\rm el}(\hat{\mathbf{k}})]c_1\,, \tag{8}$$

where $f''=\partial^2f/\partial c^2$. The effective temperature shift $\tau_{\rm el}(\hat{\mathbf{k}})$ arises from the elastic field and depends on the direction $\hat{\mathbf{k}}=k^{-1}\mathbf{k}$ of the wave vector.[1,2,8–10] Its com-

plete expression was given in Refs. 8 and 9 with c-dependent moduli and general A_{ij}. For simplicity we expand $\tau_{el}(\hat{\mathbf{k}})$ in powers of the elastic anisotropy $\xi_a \equiv (C_{11}-C_{12}-2C_{44})/C_{44}$ and the concentration-expansion coefficient $C_{44}^{\prime}$ for the shear modulus C_{44}. To first orders in ξ_a and $C_{44}^{\prime}$, we find a very natural form

$$\tau_{el}(\hat{\mathbf{k}}) = \text{const} + \tfrac{1}{2}\tau_a \sum_{i\neq j} \hat{k}_i^2 \hat{k}_j^2 + g \sum_{i,j} S_{ij}\hat{k}_i\hat{k}_j + \cdots , \quad (9)$$

where the first term is a constant independent of $\hat{\mathbf{k}}$, $\tau_a = 2a^2 C_{44}\xi_a/(C_{11}+2C_{44})^2$, and $g = -2aC_{44}^{\prime}/(C_{11}+2C_{44})$. The S_{ij} is the following symmetric traceless tensor,

$$S_{ij} = A_{ij} + A_{ji} - \frac{2}{d}\delta_{ij}\sum_j A_{jj} , \quad (10)$$

where d is the spatial dimensionality of the system. The second term of (9) arises from the cubic elastic anisotropy and the third term from the external anisotropic stress.

To describe late stages of the phase separation the quartic term ($\propto c^4$) in the free energy [or the cubic term in

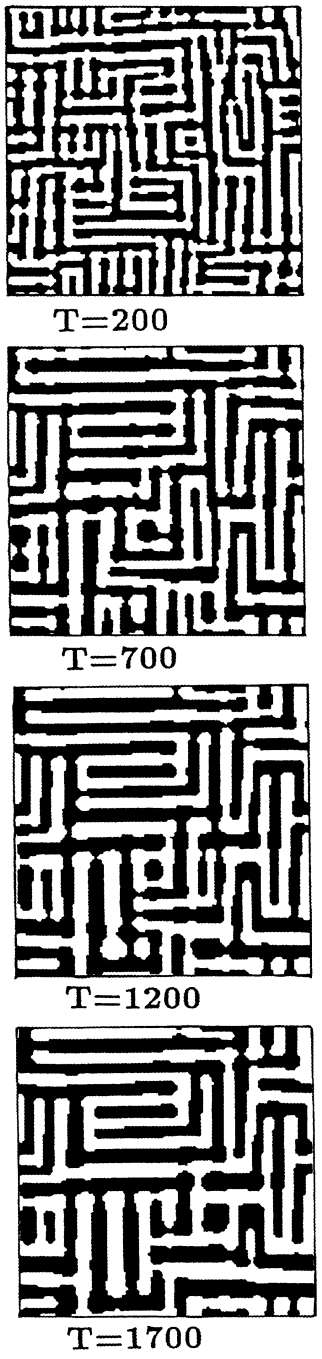

FIG. 1. Evolution patterns in cubic alloys at $\phi = \frac{1}{2}$ without external stresses. The numbers below the figures are the times after the quench.

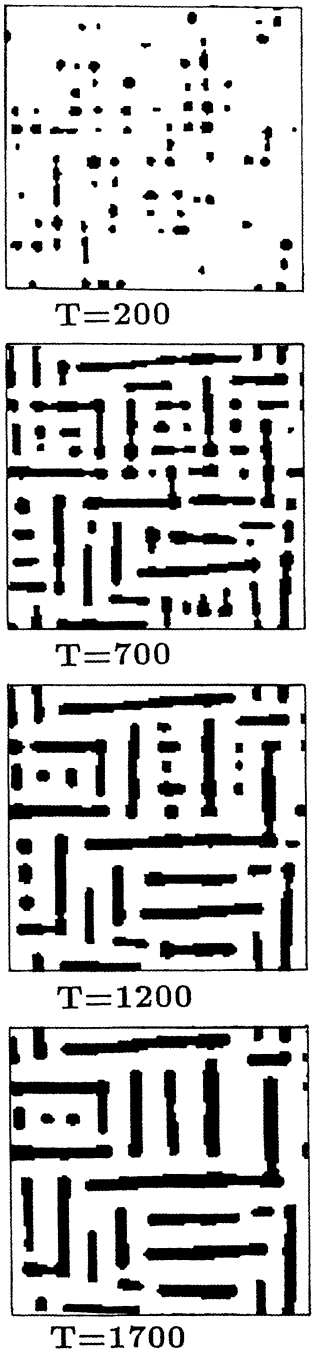

FIG. 2. Evolution patterns in cubic alloys at $\phi = 0.3$ without external stresses.

(7)] is indispensable. We hence set up the following model in the real-space representation,[9]

$$\frac{\partial}{\partial t}c=\lambda\nabla^2(\tau_0-\nabla^2+c^2)c+\tfrac{1}{2}\lambda\tau_a\sum_{i\neq j}\nabla_i^2\nabla_j^2 w$$
$$+\lambda g\sum_{i,j}S_{ij}\nabla_i\nabla_j c\,, \tag{11}$$

where $\nabla_i\equiv\partial/\partial x_i$ and w is related to the deviation $c-\langle c\rangle$ by

$$\nabla^2 w=c-\langle c\rangle\,. \tag{12}$$

The first term on the right-hand side is the usual term, τ_0 being the reduced temperature. As explained in the derivation of (9), the second and third terms of (11) are obtainable for the case,

$$|\xi_a|=|C_{11}-C_{12}-2C_{44}|/C_{44}\ll 1 \text{ and } |C_{44}^{\dagger}\gamma|\ll|a|\,, \tag{13}$$

where γ is the characteristic strain (approximately the largest component of S_{ij}). We expect that the last two terms of (11) can reproduce salient features brought about by the cubic anisotropy and the external stress. To be precise, however, a systematic perturbation theory beyond the linear scheme shows that there appears a cubic term proportional to $C_{44}^{\dagger}$ in the free energy after elimination of the elastic field.[8,9] It corresponds to an interaction introduced by Eshelby[11] and can significantly influence the morphology. In this paper we focus our attention on the effects of the last two terms of (11) and defer analysis of Eshelby's interaction to future work.

We numerically solve (11) in two space dimensions by setting $\lambda=1$, $\tau_0=-1$, and $\tau_a=0.675$ after quenching at $t=0$. Both the mesh size and time step are unity and the system is a 128×128 square lattice with the periodic boundary condition. As the initial configuration, values of c at sites are random numbers uniformly distributed between ±0.3 around a given mean value. The second term ($\propto\tau_a$) of (11) becomes $\tau_a\nabla_x^2\nabla_y^2 w=\tau_a\nabla_x^2\nabla_y^2\nabla^{-2}c$ for $d=2$, ∇^{-2} being the inverse operator of ∇^2. As a strategy to calculate this term, we solve the diffusion equation $\partial\mu/\partial t'=D(\nabla^2\mu-\nabla_x\nabla_y c)$ from $t'=0$ to 20 with $D=\frac{1}{3}$ where each given $c(\mathbf{r},t)$ is held fixed. We then substitute this result into (11) expecting $\mu\cong\nabla^{-2}\nabla_x\nabla_y c=\nabla_x\nabla_y\omega$ for large t'. As regards the integration of (11) we use Oono and Puri's method[12] and, at each mapping $t=n$, we solve the above diffusion equation.[13] The softest directions are [10] and [01] if no external stress is applied. Figures 1 and 2 show the growth of domains without external stresses at a critical quench, $\phi=\frac{1}{2}$, and an off-critical quench, $\phi=0.3$, respectively. Domains are rectangular stripes aligned in [10] or [01]. The length of the shorter sides has a sharp distribution peaked at a length $R_c(t)$, while the length of the longer sides is broadly distributed. The characteristic features agree with experiments[1] and the simulation.[4] Figure 3 displays the formation of lamellar structures under a uniaxial stress of $gS_{xx}=-gS_{yy}=-0.15$ at $\phi=\frac{1}{2}$. The layer separation is sharply distributed around $R_u(t)$. In Fig. 4 we apply a shear stress of $gS_{xy}=-0.225$ at $\phi=\frac{1}{2}$. Note that (9) becomes

$$\tau_{el}(\hat{\mathbf{k}})=\text{const}+\tau_a(\hat{k}_x\hat{k}_y)^2+2gS_{xy}(\hat{k}_x\hat{k}_y)+\cdots$$

for the case of pure shear stress and its minimization gives the softest directions. We notice that, if $\tau_a>0$ and

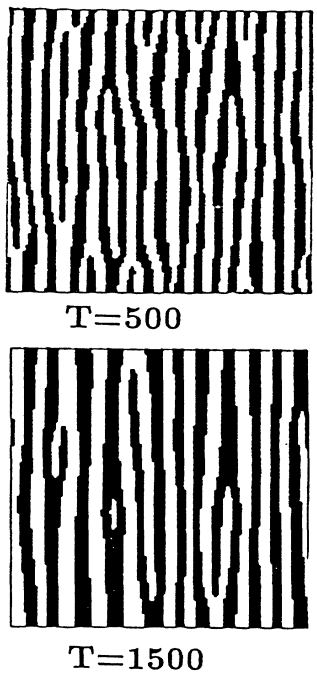

FIG. 3. Lamellar patterns under uniaxial stress. The system is compressed or stretched along [10].

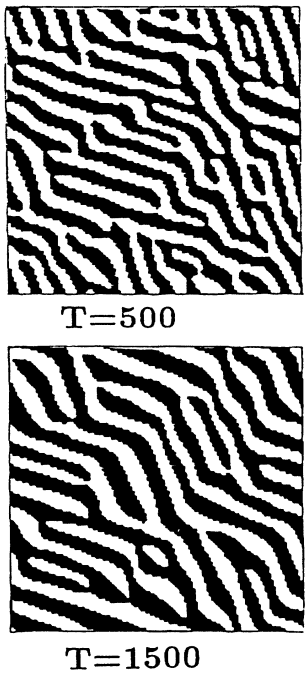

FIG. 4. Patterns under shear stress. The system is softest in the two directions making angles of 21° and 69° with respect to the horizontal axis. These patterns change into lamellar patterns for larger shear stresses.

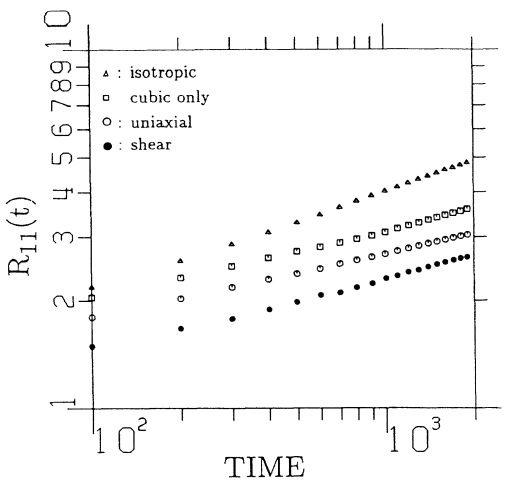

FIG. 5. Coarsening of $R_{11}(t)$ for the cubic case without external stress (□), the uniaxial case (○), the shear case (●), and the isotropic case (△). The three anisotropic cases correspond to Figs. 1, 3, and 4.

$2|gS_{xy}| < \tau_a$, there still exist two such directions making angles of θ_0 and $\pi/2-\theta_0$ with respect to the x axis where θ_0 is determined by $\sin(2\theta_0) = -2gS_{xy}/\tau_a$. The parameters in Fig. 4 are in this region with $\theta_0 \cong 21°$. However, our two-dimensional system becomes softest in only one direction, $[1\bar{1}]$ for $gS_{xy} > 0$ and $[11]$ for $gS_{xy} < 0$, in the other regions of τ_a and gS_{xy} and this is the normal direction to resultant lamellar structures. The unique patterns in the shear case are produced by competition between the cubic anisotropy and the external shear. Note that most attention so far has been paid to the uniaxial case.[3,4]

In Fig. 5 we calculate the mean size $R_{11}(t)$ in the [11] direction at $\phi = \frac{1}{2}$ by averaging over all the lines passing through sites in the [11] direction. It is nearly proportional to the inverse peak wave number for the structure factor in the [11] direction. In particular, $R_{11}(t) \cong 2^{1/2} R_c(t)$ or $2^{1/2} R_u(t)$ in the cubic or uniaxial case. The effective exponent $a \equiv d[\ln R_{11}(t)]/d(\ln t)$ behaves as follows: $a \cong 0.15$ in an early stage, $t \lesssim 300$, in all the three anisotropic cases. For later times $t \gtrsim 500$, we have found $a \cong 0.17$ for the uniaxial case and $a \cong 0.2$ for the other two cases. On the other hand, by setting $\tau_a = g = 0$, we have obtained an excellent fitting, $R_{11}(t) \propto t^{1/3}$, for the isotropic case.[12] The slower coarsening in the anisotropic cases originates from appearance of lamellarlike regions, where the interface motion is observed to be much slower than near the ends of long stripes. However, we have no appropriate theory leading to $a \sim 0.2$ at present.

We can thus examine various patterns produced by the elastic interactions using the model (11), which is much simpler than the microscopic model in the Monte Carlo simulation.[4] More quantitative analysis will be reported in the near future.

[1]A. G. Khachaturyan, *Theory of Structural Transformations in Solids* (Wiley, New York, 1983), and references therein.

[2]J. W. Cahn, Acta Metall. **10**, 179 (1962).

[3]As an experimental paper see, for example, T. Miyazaki, K. Nakamura, and H. Mori, J. Mater. Sci. **14**, 1827 (1979). Most theories in metallurgy have been energetic considerations and not dynamical ones. See, for example, W. C. Johnson, M. B. Berkenpas, and D. E. Langhlin, Acta Metall. **36**, 3149 (1988).

[4]J. Gayda and D. J. Srolovitz, Acta Metall. **37**, 641 (1989).

[5]P. W. Voorhees, J. Stat. Phys. **38**, 231 (1985).

[6]J. D. Gunton, M. San Miguel, and P. S. Sahni, in *Phase Transitions and Critical Phenomena,* edited by C. Domb and J. L. Lebowitz (Academic, New York, 1983), Vol. 8.

[7]K. Binder, in *Phase Transformations in Materials,* edited by P. Haasen (VCH Verlagesellschaft, Weinheim, Germany, 1989).

[8]A. Onuki, J. Phys. Soc. Jpn. **58**, 3065 (1989); **58**, 3069 (1989).

[9]A. Onuki, in *Formation, Dynamics, and Statistics of Patterns,* edited by K. Kawasaki, M. Suzuki, and A. Onuki (World Scientific, Singapore, 1990).

[10]H. Yamanouchi and D. de Fontaine, Acta Metall. **27**, 763 (1979).

[11]A. J. Adrell, R. B. Nicholson, and J. D. Eshelby, Acta Metall. **14**, 1295 (1966).

[12]Y. Oono and S. Puri, Phys. Rev. A **38**, 434 (1988).

[13]Let $c_n(\mathbf{k})$ and $\mu_n(\mathbf{k})$ be the Fourier components of $c(\mathbf{r},t)$ and $\mu(\mathbf{r},t)$ at the nth mapping $t = n$. Solving the diffusion equation we find $\mu_{n+1}(\mathbf{k}) = \zeta\mu_n(\mathbf{k}) + (1-\zeta)\hat{k}_x\hat{k}_y c_n(\mathbf{k})$ with $\zeta = \exp(-Dk^2t')$. We should examine how the finiteness of ζ affects the iteration scheme. We can do this task, if the mapping of c is also linearized, to find that the effect of nonvanishing ζ is negligible as long as $t' \gg 1$ even for $Dk^2t' \ll 1$. From this we expect that the choice of $t' = 20$ should be sufficient even in our nonlinear case.